

# Cellular Localization and Functional Role of Phosphatidylcholine-Specific Phospholipase C in NK Cells

Carlo Ramoni,<sup>1\*</sup> Francesca Spadaro,\* Michela Menegon,\* and Franca Podo<sup>†</sup>

Although several classes of phospholipases have been implicated in NK cell-mediated cytotoxicity, no evidence has been reported to date on involvement of phosphatidylcholine-specific phospholipase C (PC-PLC) in NK activation by lymphokines and/or in lytic granule exocytosis. This study demonstrated the expression of two PC-PLC isoforms ( $M_r$  40 and 66 kDa) and their IL-2-dependent distribution between cytoplasm and ectoplasmic membrane surface in human NK cells. Following cell activation by IL-2, cytoplasmic PC-PLC translocated from the microtubule-organizing center toward cell periphery, essentially by kinesin-supported transport along microtubules, while PC-PLC exposed on the outer cell surface increased 2-fold. Preincubation of NK cells with a PC-PLC inhibitor, tricyclodecan-9-yl-xanthogenate, strongly reduced NK-mediated cytotoxicity. In IL-2-activated cells, this loss of cytotoxicity was associated with a decrease of PC-PLC exposed on the cell surface, and accumulation of cytoplasmic PC-PLC in the Golgi region. Massive colocalization of PC-PLC-rich particles with perforin-containing granules was found in the cytoplasm of NK-activated (but not NK-resting) cells; both organelles clustered at the intercellular contact region of effector-target cell conjugates. These newly detected mechanisms of PC-PLC translocation and function support an essential role of this enzyme in regulated granule exocytosis and NK-mediated cytotoxicity. *The Journal of Immunology*, 2001, 167: 2642–2650.

Natural killer cells, a CD3<sup>-</sup>CD16<sup>+</sup>CD56<sup>+</sup> subset of large granular human lymphocytes, are able to induce both direct and Ab-mediated cellular cytotoxicity on a variety of targets, notably tumor, virus-infected, and immature hemopoietic cells (1). NK-induced cytotoxicity involves rapid effector-target cell conjugation, followed by exocytosis of granules containing perforins, serine esterases, and proteoglycans, whose release from the effector cell (degranulation) leads to the lysis of NK-sensitive or Ab-coated target cells (2). Upon activation by lymphokines, NK cells acquire the capability of killing a wider range of targets, including tumor cells resistant to freshly isolated NK cells.

NK cell functions are triggered by the activation of multiple biochemical pathways, associated with specific, still only partially elucidated, signal transduction events (1, 3). Particular attention has been focused on the activation of phospholipases of the C, D, and A<sub>2</sub> type, implicated in the regulation of NK cytotoxicity through the generation of multiple, sometimes interconvertible lipid second messengers (4–6). Among these, phosphatidylinositol 4,5-bisphosphate-specific phospholipase C (PIP<sub>2</sub>-PLC)<sup>2</sup> is rapidly activated by cross-linking of low affinity IgG FcR (FcγRIII or CD16II) during NK-mediated cytotoxicity (7–10), with generation of two second messengers, inositol 1,4,5-trisphosphate and 1,2-diacylglycerols (DG), which respectively induce intracellular calcium mobilization and protein kinase C activation. Receptor-me-

diated phosphatidylcholine-specific phospholipase D (PC-pld) activation has been reported to occur independently of the PIP<sub>2</sub> turnover in NK-stimulated cells, through cell surface-associated molecules, including CD16 (5, 11, 12). This pathway produces phosphatidate and, in a subsequent hydrolysis step, DG, second messengers implicated in the biosynthesis and secretion of TNF-α (11). Moreover, the use of pharmacological inhibitors demonstrated that PC-pld activation is also an important step in the CD16-triggered signal cascade that leads to NK cytotoxic granule exocytosis (12).

Finally, cross-linking of CD16 receptors triggers, in activated NK cells, the induction of both cytosolic and secretory phospholipase A<sub>2</sub> isoforms. These enzymes, responsible for arachidonic acid production and subsequent generation of platelet-activating factor and leukotrienes (13, 14), are also involved in the release of cytotoxic granules, at least in some mammalian species (15).

More limited evidence has been reported on the possible involvement in NK cell cytotoxicity of neutral-active PC-specific phospholipase C (PC-PLC), major enzyme of the PC cycle, held responsible for the production of non-PIP<sub>2</sub>-derived DG in a number of receptor-stimulated cells, including lymphocytes (16–22).

Indirect evidence in support of a possible role of PC-PLC in NK-mediated cell killing was provided by the dose-dependent inhibition exerted on the lytic activity of isolated cytotoxic granules by free phosphocholine (PCho), a product of PLC-mediated PC hydrolysis (23). This compound, which represents the predominant headgroup esterified to phospholipids on the outer leaflet of the plasma membrane of eukaryotic cells, was the most potent inhibitor of granule cytolytic activity among various phosphomonoesters (e.g., glycerophosphate, phosphoethanolamine) or non-phosphorylated derivatives of phospholipid headgroups (choline, ethanolamine). The specific inhibitory effect exerted by free PCho suggests a possible competition between the free base and PCho-containing headgroups exposed on the target cell, toward the activity of specific enzymes expressed by the effector cell. Subsequent studies by Tschopp et al. (24) demonstrated that the PCho moiety acts as Ca<sup>2+</sup>-dependent receptor for perforin on lipid membrane models (PC- and sphingomyelin-containing vesicles) and

Laboratories of \*Immunology and <sup>†</sup>Cell Biology, Istituto Superiore di Sanità, Rome, Italy

Received for publication January 10, 2001. Accepted for publication June 20, 2001.

The costs of publication of this article were defrayed in part by the payment of page charges. This article must therefore be hereby marked *advertisement* in accordance with 18 U.S.C. Section 1734 solely to indicate this fact.

<sup>1</sup> Address correspondence and reprint requests to Dr. Carlo Ramoni, Laboratory of Immunology, Istituto Superiore di Sanità, Viale Regina Elena 299, 00161 Rome, Italy. E-mail address: ramoni@iss.it

<sup>2</sup> Abbreviations used in this paper: PIP<sub>2</sub>-PLC, phosphatidylinositol 4,5-bisphosphate-specific phospholipase C; CLSM, confocal laser-scanning microscopy; D609, tricyclodecan-9-yl-xanthogenate; DG, diacylglycerol; DiOC<sub>6</sub>(3), 3,3'-dihexyloxocarbocyanine iodide; ER, endoplasmic reticulum; MTOC, microtubule-organizing center; PC, phosphatidylcholine; PCho, phosphocholine; PLC, phospholipase C; pld, phospholipase D.

also on target cell membranes. No specific studies were then addressed to investigate expression, subcellular localization, and possible functional role of PC-PLC in NK-mediated cytotoxicity.

This work provides the first evidence on: 1) presence and subcellular localization of PC-PLC isoforms in human NK cells; 2) comigration of the enzyme with perforin granules in IL-2-activated NK cells; and 3) functional role of PC-PLC in NK-mediated cell killing.

## Materials and Methods

### Chemicals and biochemicals

BSA, Triton X-100, aprotinin, Tween 20, and poly-L-lysine hydrobromide (molecular mass 400 kDa) were supplied by Sigma (St. Louis, MO). Alexa 488-conjugated 3,3'-dihexyloxacarbocyanine iodide (DiOC<sub>6</sub>(3)) was purchased from Molecular Probes (Eugene, OR). Tricyclodecan-9-yl-xanthogenate (D609) was supplied by Calbiochem (Frankfurt, Germany), and human rIL-2 by Roche (Basel, Switzerland). The ECL Western blotting system, commercialized by Amersham Life Science, was supplied by Amersham Srl (Milan, Italy).

### Antibodies

The following mAbs were utilized to identify Ags characteristic of the NK phenotype: B73.1 (IgG1, anti-CD16), kindly provided by G. Trinchieri (Wistar Institute, Philadelphia, PA); 3G8 (IgG1, anti-CD16), OKT3 (IgG2a, anti-CD3), OKT4 (IgG2, anti-CD4), OKT8 (IgG2, anti-CD8), and 63D3 (anti-CD14), produced from cells obtained from the American Type Culture Collection (ATCC, Manassas, VA); and anti-CD20, anti-CD16 PE, and anti-CD56 PE from BD Biosciences (San Jose, CA).

The following Abs were used to detect specific cell components: rabbit polyclonal anti-PC-PLC Abs raised against bacterial (*Bacillus cereus*) PC-PLC and cross-reacting with mammalian PC-PLC, obtained according to the procedure described by Clark et al. (25), modified as reported (26), and purified by absorption to and elution from protein A-Sepharose; a preparation of mixed anti-PIP<sub>2</sub>-PLC- $\gamma$ 1 mAbs, purchased from Upstate Biotechnology (Lake Placid, NY); anti-human golgin-97 mAb from Molecular Probes; anti-human perforin mAb from Calbiochem; and anti- $\beta$ -tubulin, anti-F-actin, anti-kinesin, and anti-dynein mAbs from Sigma.

The following fluorochrome-conjugated secondary Abs were utilized for indirect immunofluorescence examinations: Alexa 488- and Alexa 594-conjugated goat anti-rabbit IgG and Alexa 488-conjugated goat anti-mouse IgG F(ab')<sub>2</sub> fragment, purchased from Molecular Probes.

### Cell lines

Cell lines K562 (human erythroleukemia), U937 (human monocytic leukemia), DAUDI (human lymphoblastoid leukemia), and the EBV-transformed B cell line RPMI 8866 were obtained from the ATCC. These cell lines, as well as Ab-secreting hybrid cell lines (OKT3, OKT4, OKT8, and 63D3), were routinely seeded from larger cultures into 25-cm<sup>2</sup> tissue culture flasks (Falcon) at a density of 1–4  $\times$  10<sup>5</sup> cells/ml RPMI 1640, supplemented with 10% heat-inactivated (56°C, 30 min) FCS from Life Technologies (Italia, Milan, Italy), 2 mM glutamine, 100 U/ml penicillin, and 100 mg/ml streptomycin. Cells were grown at 37°C, under 7% CO<sub>2</sub> atmosphere, in a conventional water-jacketed incubator. The cells were harvested at the mid-log phase of growth. All cell lines were *Mycoplasma* free, as controlled by repetitive testing with Hoechst fluorescent staining of cytoplasmic DNA. Cell viability, assessed by trypan blue exclusion test, was  $\geq$ 98%.

### Fresh human NK cell preparation

Human PBMCs were isolated from buffy coats of normal donors by His-topaque-1077 (Sigma) gradient, centrifuged, and passed through nylon wool columns (Robbins Scientific, Sunnyvale, CA). The NK cells were further purified by rigorous negative immunomagnetic selection. Briefly, anti-CD3-, anti-CD4-, anti-CD8-, anti-CD20-, and anti-CD14-pretreated cells were further incubated by using magnetic particles coated with F(ab')<sub>2</sub> anti-mouse IgG (Dynal, Oslo, Norway). After this second step, the resulting NK cell population was over 90% CD16<sup>+</sup>, CD56<sup>+</sup>, CD3<sup>-</sup>, and CD14<sup>-</sup>, as assessed by cytofluorometric analysis (cell viability  $\geq$ 99%).

### Long-term human NK cell preparation and activation by IL-2

Long-term NK cells were obtained by coculturing non-nylon-adherent human PBMCs from buffy coats (4  $\times$  10<sup>5</sup> cells/ml) with irradiated (4000 rad) RPMI 8866 (1  $\times$  10<sup>5</sup> cells/ml) at 37°C in a humidified 7% CO<sub>2</sub> atmosphere

for 10 days, as previously described (27). On day 10, the contaminating T cells were eliminated by indirect negative immunomagnetic depletion by mixed anti-CD3, anti-CD4, and anti-CD8 mAbs (as described above for fresh NK cells), and the resulting cell population was  $>$ 95% pure, as assessed by cytofluorometric analysis.

For activation, long-term NK cells were incubated with human rIL-2 (100 U/ml) for 3 days, starting on day 7 of culture. Cell activation was associated with an increase in cell number ranging between 1.2 and 2.3 $\times$ , according to the donor (27). These cell preparations will be referred to as NK-activated cells. Both control and NK-activated cells were over 95% viable.

### Immunofluorescence epimicroscopy and flow cytometry analyses

The surface phenotype of cells in suspension and PC-PLC expression in either fixed or unfixed NK cells were characterized by indirect immunofluorescence, by using either mAbs or polyclonal Abs. Briefly, 5  $\times$  10<sup>5</sup> cells were added per well in a U-bottom microtiter plate and washed once with PBS containing 0.2 mM Na<sub>3</sub>N and 1% BSA (PBS-Na<sub>3</sub>N-BSA). Cells were sequentially incubated (30 min, 4°C) with appropriate dilutions of the primary Ab, washed twice with PBS-Na<sub>3</sub>N-BSA, and incubated for 30 min at 4°C with the appropriate fluorochrome-conjugated secondary (either goat anti-mouse or goat anti-rabbit) Abs, as specified for each series of experiments. The control samples, consisting of a portion of the same NK cell preparation incubated only with the secondary Alexa-conjugated Ab, were treated in the same way. After extensive washes, cell fluorescence intensity was measured on logarithmic scale using a flow cytometer FAC-Scan (BD Biosciences). For immunofluorescence microscopy analyses, the cells were Cytospin sedimented on a glass slide, fixed, and permeabilized with cold methanol (~20°C, 10 min) and 0.2% Triton X-100 in PBS (5 min, room temperature), and then incubated for immunofluorescence, as above. Finally, the ProLong (Molecular Probes) antifade reagent was added immediately before analyses on a Zeiss Axioscop fluorescence microscope (Zeiss, Oberkochen, Germany), equipped with appropriate filters.

Figures were prepared using Adobe Photoshop software (Adobe Systems, Mountain View, CA).

### Confocal laser-scanning microscopy (CLSM) analyses

For CLSM analyses, NK cells were seeded on poly-L-lysine hydrobromide-coated cover glass (10  $\mu$ g/ml, 40 min, room temperature) and allowed to attach for 90 min at 37°C. After washing with PBS, the cells were fixed by paraformaldehyde 3% (30 min, 4°C), permeabilized by Triton X-100 (0.5%, 10 min at room temperature), and then stained (30 min, 37°C) with appropriate pretested dilutions of the primary and Alexa-conjugated secondary Abs, according to the procedures described in the previous section. The extensively rinsed cover glass was then mounted on the microscope slide with the ProLong reagent, and CLSM observations were performed using a Leica TCS 4D apparatus, equipped with an argon-krypton laser, double-dichroic splitters (488/568 nm), 520-nm barrier filter for Alexa 488 (green), and 590-nm barrier filter for Alexa 594 (red) observations. Image acquisition and processing were conducted by using the SCANware and Multicolor Analysis (Leica Lasertechnik GmbH, Heidelberg, Germany) and Adobe Photoshop software programs. Signals from different fluorescent probes were taken in parallel, and colocalization was detected in white (pseudo-color). Several cells were analyzed for each labeling condition, and representative results are presented.

### Western blot analyses of PC-PLC enzyme isoforms

Cells (20  $\times$  10<sup>6</sup> per sample) were resuspended in 50  $\mu$ l lysis buffer (100 mM Tris-HCl, pH 8, 150 mM NaCl, 1% Triton X-100, 1% aprotinin, 250 mM PMSF) for 30 min. All subsequent manipulations were performed at ice-melting temperature. Lysates were cleared of nuclei and detergent-insoluble materials by 20-min centrifugation at 15,000  $\times$  g. The samples were then resuspended in 20  $\mu$ l reducing buffer, boiled, and resolved by 7% SDS-PAGE, using a mini-Protein II apparatus (Bio-Rad Laboratories, Hercules, CA), and transferred to nitrocellulose in a Bio-Rad *trans* blot apparatus. Blots were washed two to three times for 5–10 min in TBS buffer, containing 0.05% Tween 20 (TBS-T), and blocked in 5% nonfat dry milk in PBS-T for 60 min. After three washes in TBS-T, blots were incubated with rabbit anti-PC-PLC Abs. Enzyme isoforms were detected using an anti-rabbit HRP-conjugated secondary Ab and the ECL Western blotting reagent system.

### Cellular cytotoxicity assay

The cytolytic activity of resting or IL-2-activated NK cells was tested against either NK-sensitive (K562, U937) or NK-resistant (DAUDI) leukemia cell lines by a classical 3-h <sup>51</sup>Cr release assay. The percentage of

specific  $^{51}\text{Cr}$  release was calculated as follows: (experimental release – spontaneous release)/(maximum release – spontaneous release)  $\times$  100 (27). The effects of PC-PLC inhibition on NK-mediated cytotoxic activity were tested on NK cells isolated from different donors, preincubated in the presence of D609 (15–60  $\mu\text{g}/\text{ml}$ ) for different time intervals (as specified), extensively washed, and then tested for cellular cytotoxicity against target leukemia cells. In these experiments, the inhibitor did not induce any significant modification on NK cell viability (>90% by trypan blue exclusion test), nor on cell distribution in different phases of the cell cycle; in particular, the apoptotic fraction (sub- $G_0$  peak) was always below detection level.

## Results

### Immunofluorescence detection of PC-PLC in intact NK cells

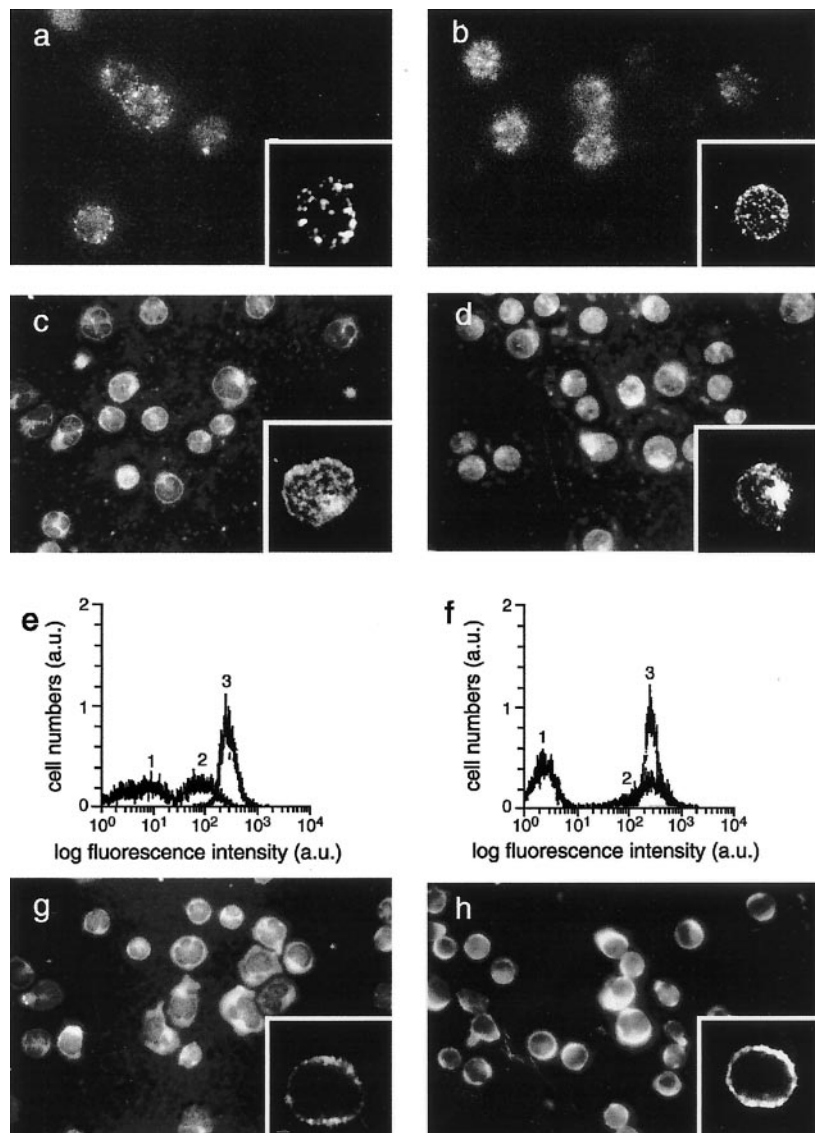
Indirect immunofluorescence analyses of either unfixed or fixed and permeabilized NK-resting cells, preincubated with anti-PC-PLC Abs (26), demonstrated that PC-PLC was expressed both on the outer cell surface (Fig. 1*a*) and within cytoplasmic compartments (Fig. 1*c*). CLSM analyses allowed a more detailed insight on the spotlike distribution of PC-PLC exposed on the external cell surface (Fig. 1*a*, *inset*), while intracellular PC-PLC appeared to be generally localized within defined cytoplasmic regions (Fig. 1*c*). This aspect will be analyzed in more detail by CLSM, as described below.

Similar subcellular PC-PLC distribution patterns were observed in NK-activated cells (Fig. 1, *b* and *d*), which, however exhibited, as compared with NK-resting cells, a substantial increase in the relative amount of PC-PLC exposed on the outer cell surface. Moreover, the pattern of membrane-bound fluorescence appeared to be clustered in smaller particles.

Flow cytometry analyses allowed quantification of these observations, in terms of distribution and relative intensity of indirect immunofluorescence, in either fixed or unfixed cells. The overall fluorescence intensity of fixed and permeabilized cells appeared rather homogeneous (as demonstrated by the sharp *peak 3* in Fig. 1, *e* and *f*), with a mean value not substantially modified by IL-2 activation. This result indicated that the total amount of expressed PC-PLC was practically the same in NK-resting and in NK-activated cells. Flow cytometry analyses of unfixed cells showed, instead, a rather broader fluorescence distribution of PC-PLC exposed on the outer cell surface (Fig. 1, *e* and *f*, *peak 2*), with a mean value over two times higher in NK-activated than in NK-resting cells.

The subcellular distribution of PC-PLC in NK cells was compared with that of  $\text{PIP}_2$ -specific phospholipase C- $\gamma 1$ , major PLC isoform, responsible for receptor-mediated activation of

**FIGURE 1.** Expression and subcellular localization of PC-PLC in NK cells. Indirect immunofluorescence analyses were performed on NK-resting (*left panels*) or IL-2-activated NK cells (*right panels*). PC-PLC was detected in either unfixed (*a* and *b*) or fixed cells (*c* and *d*), using rabbit polyclonal anti-PC-PLC Abs and Alexa 594 goat anti-rabbit IgG (H + L) as secondary Ab. *e* and *f*, Immunofluorescence flow cytometry analyses of cells prepared as in *a–d*. The mean fluorescence intensity values were:  $2 \times 10^2$  in either resting or activated fixed cells (*peak 3*);  $0.9 \times 10^2$  in unfixed NK-resting cells and  $2 \times 10^2$  in unfixed NK-activated cells (*peak 2*). a.u., arbitrary units. Control cells were incubated with the secondary Ab only (*peak 1*). These results were confirmed by five independent series of experiments. The *bottom panels* show the subcellular distribution of  $\text{PIP}_2$ -PLC- $\gamma 1$  in fixed NK-resting (*g*) and NK-activated cells (*h*), as detected by immunofluorescence, using mixed anti- $\text{PIP}_2$ -PLC- $\gamma 1$  (primary) mAbs and Alexa 488-conjugated goat anti-mouse IgG F(ab') $_2$  as secondary probe. *Insets*, Typical examples of CLSM analyses on the cell preparations examined in the respective panels.





the phosphoinositide cycle. Epifluorescence and CLSM experiments demonstrated that the subcellular distribution of PC-PLC was substantially different from that of PIP<sub>2</sub>-PLC- $\gamma$ 1, whose fluorescent pattern was less granular and mostly confined to subcortical areas of the plasma membrane, especially in NK-activated cells (Fig. 1, *g* and *h*).

In conclusion, epifluorescence, CLSM, and flow cytometry experiments demonstrated that PC-PLC was expressed both in cytoplasmic compartments and on the outer cell surface of either resting or activated NK cells. The fraction of PC-PLC exposed on the cell surface increased over 2-fold, upon IL-2-mediated cell activation. The subcellular distribution of PC-PLC was substantially different from that of PIP<sub>2</sub>-PLC- $\gamma$ 1.

#### Detection of PC-PLC in NK cell lysates

Western blot analyses on NK cell lysates showed two sharp protein bands (Fig. 2), specifically recognized by the same anti-PC-PLC Abs utilized for the immunofluorescence experiments described in the previous section. These protein bands, corresponding to  $M_r$  values of 66 and 40 kDa, respectively, were attributed to different PC-PLC isoforms. The relative amount of the two isoforms showed some variability from donor to donor, but was not significantly altered by IL-2 activation. Preincubation of NK-activated cells with the PC-PLC inhibitor D609 (17, 22, 28, 29) did not induce any substantial modification in the expression of the two PC-PLC isoforms.

The same PC-PLC isoforms were also detected in some leukemia cells, such as K562 and DAUDI (Fig. 2). Only the 40-kDa isoform was instead detected in U937 cells, in close agreement with a previous study by Clark et al. (25), while the 66-kDa isoform alone has been previously reported by our group in murine embryo-derived NIH-3T3 fibroblasts and in their *H-ras* transformants (26).

In conclusion, two PC-PLC isoforms are expressed, with some interdonor variability, in lysates of either resting or activated NK lymphocytes.

#### Localization of PC-PLC in cytoplasmic organelles of NK cells

To gain more detailed information on the cytoplasmic localization of PC-PLC, dual immunofluorescence CLSM analyses were performed on fixed NK-resting or NK-activated cells, preincubated with both anti-PC-PLC Abs (detected in red) and probes specific for different cytoplasmic organelles (detected in green). In particular, examinations were performed using either DiOC<sub>6</sub>(3) (30), at

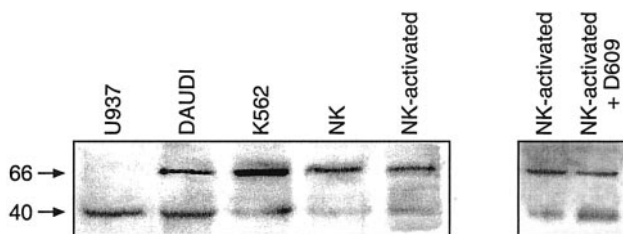


**FIGURE 2.** Detection of PC-PLC isoforms in human NK cell lysates. Immunoblotting experiments were conducted on total lysates of NK-resting or NK-activated cells, either untreated or preincubated with D609 (50 μg/ml, 180 min) and then extensively washed. Immunoblots of lysates of the tumor U937, DAUDI, and K562 cell lines are also shown for comparison. Arrowheads indicate the apparent molecular mass (kilodaltons) of PC-PLC isoforms detected by the same anti-PC-PLC Abs utilized in Fig. 1 (*a-f*). Similar results were obtained in three series of independent experiments. For further details on the Western blot analyses, see *Materials and Methods*.

a concentration (1 μg/ml) at which it acts as specific marker of endoplasmic reticulum (ER), or anti-golgin mAb, a specific probe for the Golgi apparatus. The experiments demonstrated colocalization (white) of PC-PLC with the ER (Fig. 3A), mainly within the Golgi apparatus (Fig. 3C) in NK-resting cells. A much more extended colocalization of PC-PLC with the ER marker was observed in NK-activated cells (Fig. 3B), in which the enzyme was not exclusively confined to the Golgi region (Fig. 3D).

#### Colocalization of PC-PLC with cytoskeleton components and motor proteins

Dual fluorescence CLSM analyses performed on fixed NK-resting cells, double-stained with anti-PC-PLC Abs (red) and anti- $\beta$ -tubulin mAbs (green), demonstrated some colocalization of PC-PLC with the microtubule-organizing center (MTOC) (Fig. 4A). In NK-activated cells, not only did this colocalization become much more pronounced, but several PC-PLC-enriched particles were also found to colocalize with microtubule filaments (Fig. 4B).

Furthermore, CLSM analyses on NK-activated cells double-stained with anti-PC-PLC and anti-kinesin (Fig. 4C) or anti-dynein (Fig. 4D) Abs showed that PC-PLC was apparently transported away from the MTOC region toward the cell periphery, mainly by the motor protein kinesin, rather than by dynein.

Finally, a substantial colocalization of PC-PLC with F-actin filaments was observed in NK-activated (Fig. 4F), but not in NK-resting cells (Fig. 4E).

It is interesting to note that intracellular PC-PLC was not exclusively confined to cytoplasmic regions, since several PC-PLC-enriched particles were also detected in the nucleus. This phenomenon, particularly evident in Fig. 4C, seems worthy of further investigation, also in the light of increasing evidence pointing to the presence of phospholipases of the C type (specific for either PIP<sub>2</sub> or PC) in the nucleus of several cell lines, where these enzymes are proposed to exert key regulatory functions (31–33).

#### Association of cytoplasmic PC-PLC with perforin-containing granules

CLSM analyses of fixed NK-resting cells (Fig. 5A) demonstrated that PC-PLC (red) and perforin-carrying granules (green) exhibited some areas of colocalization (white), especially in the Golgi region. Both types of particles were much more widely distributed throughout the cytoplasm of NK-activated cells, with extensive colocalization (Fig. 5B). It is interesting to note that in the latter cells, most of the perforin-carrying granules were associated with PC-PLC, but not all PC-PLC particles colocalized with perforin molecules.

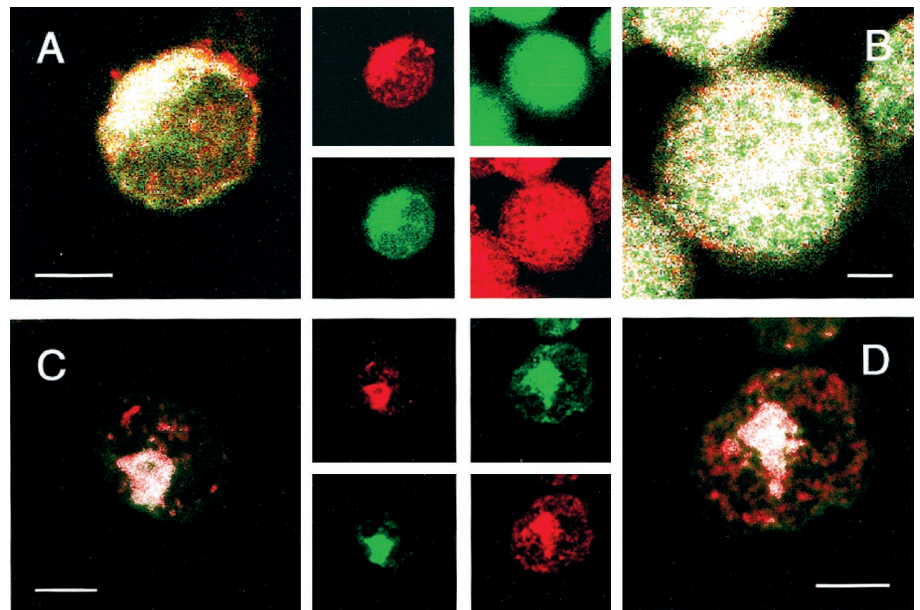
In NK-activated cells preincubated with D609, both PC-PLC and perforin granules were confined to the Golgi region, where they closely colocalized (Fig. 5C).

Finally, when NK-activated cells were induced to form conjugates with either NK-sensitive (K562) or NK-resistant (DAUDI) target cells, a massive colocalization of PC-PLC and perforin granules occurred at the intercellular contact region (Fig. 5, *D* and *E*). This phenomenon was, instead, generally absent in conjugates of NK-resting cells with either type of target (data not shown).

#### Effects of the PC-PLC inhibitor D609 on NK-mediated lytic activity

To further investigate the functional role of PC-PLC in the cytotoxic process, experiments were performed on purified long-term cultured NK cells (from different donors), preincubated with D609 (0, 15, 30, 45, or 60 μg/ml; 15 min) before lytic assays against the NK-sensitive K562 target cells (E:T cell ratio, *r*, between 1.6:1 and 12.5:1). Three independent series of experiments (example in Fig.

**FIGURE 3.** Colocalization of PC-PLC with cytoplasmic organelles (ER and Golgi components) in NK cells. Dual fluorescence CLSM analyses were performed on fixed NK-resting (A and C) or NK-activated cells (B and D), double-stained with rabbit anti-PC-PLC Abs (detected in red by Alexa 594 anti-rabbit, as secondary Ab) and either the ER probe DiOC<sub>6</sub>(3) (1  $\mu$ g/ml, green fluorescence) or anti-golgin-97 mAb (detected in green by Alexa 488 goat anti-mouse, as secondary Ab). Colocalization was detected in white (pseudo-color). *Insets*, Distribution of individual components, under the respective experimental conditions adopted in each panel. Bars correspond to 5  $\mu$ m.

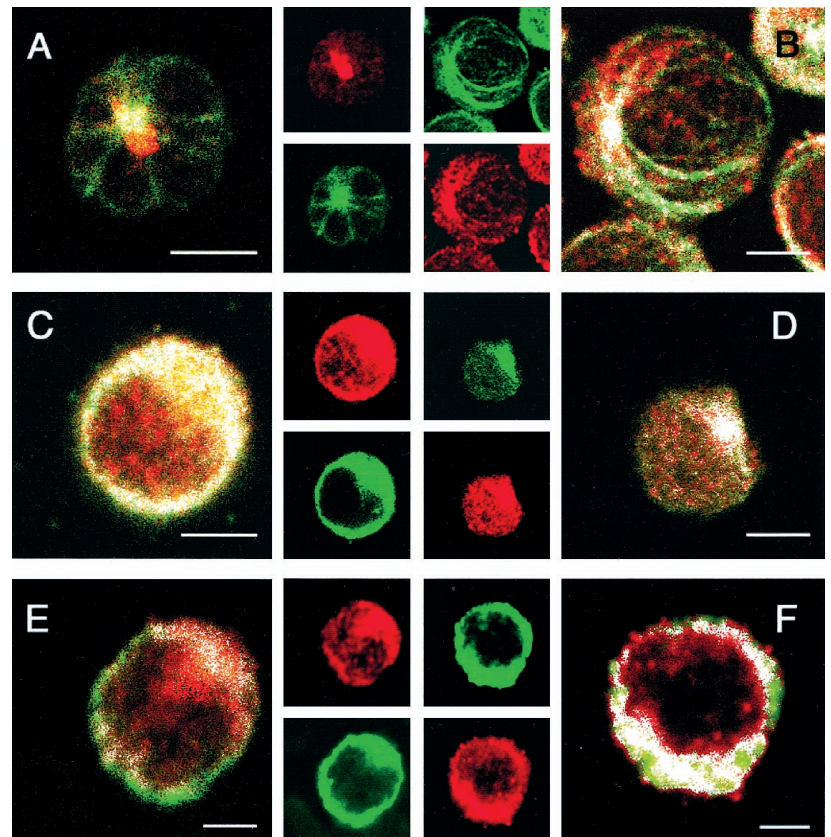


6A) consistently showed that preincubation of NK cells with D609 induced dose-dependent decreases in NK-mediated lytic activity. The percent decreases in cytotoxicity varied (according to the E:T cell ratio) from 5–15% at the inhibitor concentration,  $c = 15 \mu\text{g/ml}$  to 10–40% at  $c = 30 \mu\text{g/ml}$ ; 25–60% at  $c = 45 \mu\text{g/ml}$ ; and 30–60% at  $c = 60 \mu\text{g/ml}$ . The alterations in specific cell lysis (mean values  $\pm$  SD, seven series of independent experiments) induced by D609 (50  $\mu\text{g/ml}$ , 15 min) in long-term cultured NK cells are reported in Fig. 6B.

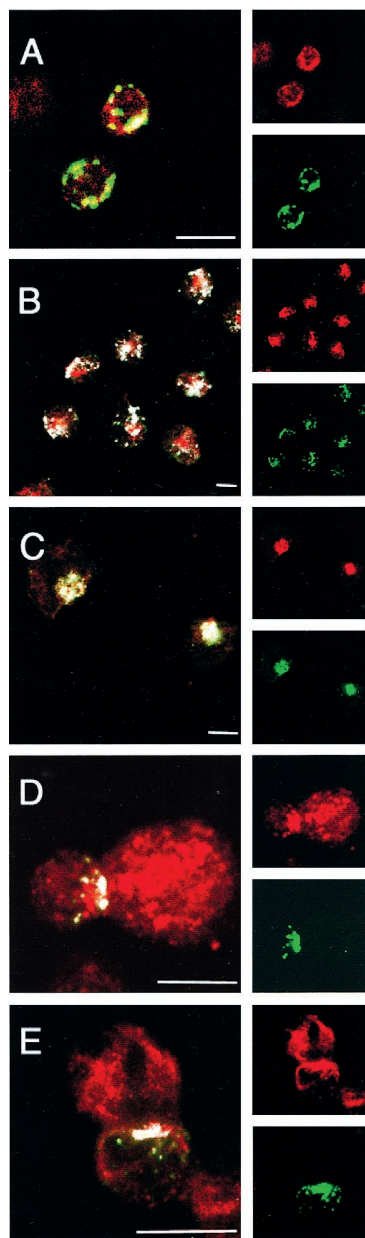
Similar effects were obtained with another NK-sensitive target cell line, U937 (data not shown).

Fig. 6C reports the results (mean values  $\pm$  SD) of four series of independent experiments conducted to assess the cytotoxic activity of NK-activated cells preincubated with D609 (50  $\mu\text{g/ml}$ , 15 min), washed, and challenged with either K562 or DAUDI cells (the latter being resistant to NK-resting but not to NK-activated cells). All these experiments demonstrated again a strong inhibition by D609 of NK-mediated cytotoxicity, with percent decreases in lytic

**FIGURE 4.** Colocalization of PC-PLC with cytoskeleton components in NK cells. Dual fluorescence CLSM analyses were conducted on fixed NK-resting (A and E) or NK-activated cells (B–D and F), double-stained with rabbit anti-PC-PLC Abs (detected in red by Alexa 594 anti-rabbit, as secondary Ab) and anti- $\beta$ -tubulin (A and B), or anti-kinesin (C), or anti-dynein (D), or anti-F-actin mAbs (E and F), all detected in green by Alexa 488 goat anti-mouse, as secondary Ab. Colocalization was detected in white (pseudo-color). *Insets*, Distribution of individual components, under the respective experimental conditions adopted in each panel. Bars correspond to 5  $\mu$ m.







**FIGURE 5.** Colocalization of PC-PLC with perforin-containing granules in NK cells. Dual fluorescence CLSM analyses were performed on fixed cells, double-stained with rabbit anti-PC-PLC Abs (detected in red by Alexa 594 anti-rabbit, as secondary Ab) and anti-perforin mAb (detected in green by Alexa 488 goat anti-mouse, as secondary Ab). Colocalization was detected in white (pseudo-color). *A*, NK-resting cells; *B*, NK-activated cells; *C*, NK-activated cells preincubated with D609 (50  $\mu\text{g}/\text{ml}$ , 180 min, 37°C); *D*, conjugate of NK activated with K562 target cell; *E*, conjugate of NK activated with DAUDI target cell. *Insets*, Distribution of individual components, under the respective experimental conditions adopted in each panel. Bars correspond to 5  $\mu\text{m}$ .

activity (with respect to untreated control cells) higher than 90% in the E:T cell ratio range between 6.2:1 and 50:1. These findings further supported a functional role of PC-PLC in the cellular mechanisms responsible for target cell lysis.

Flow cytometry analyses were finally performed on either unfixed or fixed cells to investigate whether the effects of the PC-PLC inhibitor on NK-mediated cytotoxicity were associated with alterations in the relative distribution of the enzyme between cytoplasmic and membranous compartments of NK-activated cells. Exper-

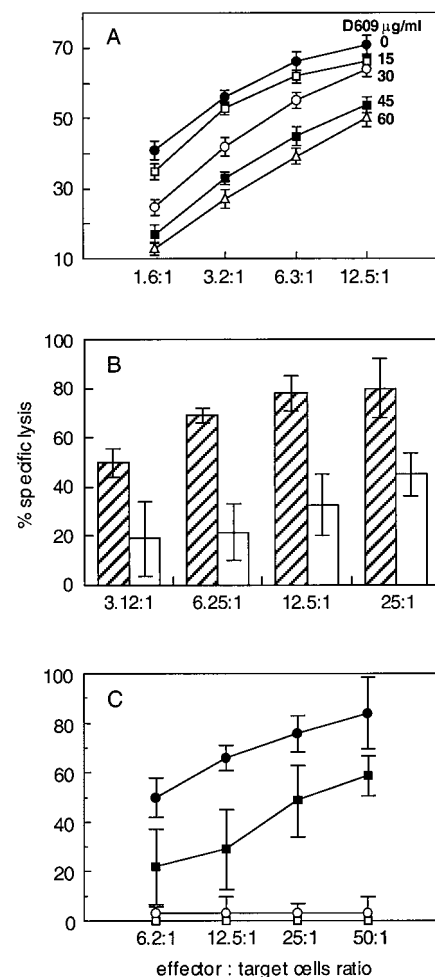


**FIGURE 6.** Inhibition by D609 of NK cytotoxicity against tumor target cells. *A*, Long-term cultured NK cells preincubated with different concentrations of D609 (0, 15, 30, 45, or 60  $\mu\text{g}/\text{ml}$ ; 15 min; 37°C) and then extensively washed, before  $^{51}\text{Cr}$  release assays against K562 target cells. Data represent the mean values  $\pm$  SD of a triplicate assay of one of three independent series of experiments with similar results. *B*, Results (mean values  $\pm$  SD) of seven independent series of experiments conducted on long-term cultured NK cells (from different donors) preincubated with D609 (50  $\mu\text{g}/\text{ml}$ , 15 min), and washed before lytic assays against K562 cells. *C*, NK-activated cells preincubated with D609 (50  $\mu\text{g}/\text{ml}$ , 15 min) and washed, before cytotoxicity assays against either NK-sensitive K562 ( $\circ$ ) or NK-resistant DAUDI cells ( $\square$ ).  $\blacksquare$  and  $\bullet$ , Respective controls. Data (mean  $\pm$  SD) were obtained from four independent series of experiments. For details on cytotoxic assays, see *Materials and Methods*.

iments on unfixed cells (Fig. 7, *bottom panel*) demonstrated that preincubation of the effector cells with D609 (50  $\mu\text{g}/\text{ml}$ ) resulted in a strong decrease in the exposure of PC-PLC on the outer cell surface, which was reduced by  $40 \pm 5\%$  after 15 min of cell preincubation with the inhibitor and by  $75 \pm 15\%$  after 180 min. On the other hand, analyses on fixed and permeabilized cells (*upper panel*) showed that the overall (cytoplasmic plus membranous) PC-PLC expression was not significantly decreased by 15-min incubation with D609 ( $6 \pm 1\%$ ) and underwent a decrease of  $40 \pm 10\%$  at 3 h. The observed alterations in PC-PLC subcellular redistribution were fully reversible 6 h after removal of the inhibitor (data not shown).

In conclusion, immunofluorescence analyses supported the notion that preincubation of NK-activated cells with the PC-PLC inhibitor D609 induces a recycling of PC-PLC isoform(s) from the

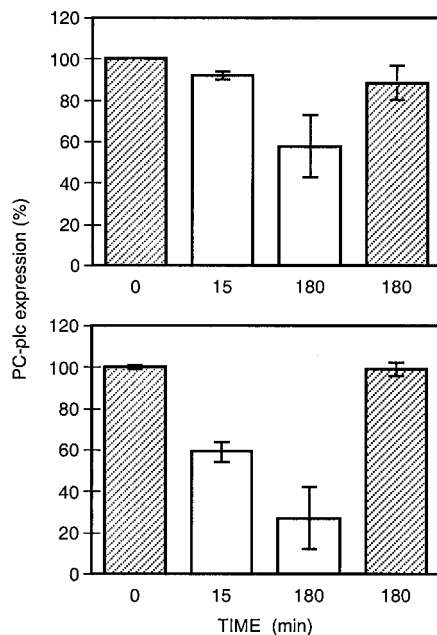


**FIGURE 7.** Effect of D609 on PC-PLC expression and subcellular localization in NK-activated cells. Immunofluorescence flow cytometry experiments were conducted on either fixed (*top*) or unfixed cells (*bottom*) preincubated with D609 (50  $\mu\text{g}/\text{ml}$ , 37°C) for either 15 or 180 min ( $\square$ ). Control cells, incubated under similar conditions in the absence of the inhibitor, were also analyzed at 0 and 180 min ( $\text{▨}$ ). The results (mean values  $\pm$  SD) were obtained from five series of independent experiments.

cell surface to intracellular compartments, without significant alteration in the total amount of PC-PLC expression at 15 min and a (reversible) decrease in the latter at longer times (up to 40% at 3 h).

## Discussion

This work reports evidence on 1) PC-PLC expression in NK cells; 2) cytokine-dependent distribution of this enzyme between cytoplasmic regions (Golgi, MTOC, ER) and the outer cell membrane surface; 3) colocalization of PC-PLC with perforin granules along microtubules in IL-2-activated cells and massive accumulation of both components at the contact region of NK-target cell conjugates; 4) subcellular redistribution of PC-PLC and inhibition of NK cytotoxicity upon cell exposure to the PC-PLC inhibitor D609. These results implicate a role of PC-PLC in NK-mediated cytotoxicity.

At the present stage, no definite hypothesis can be suggested regarding the possible differential localization and function of the two PC-PLC isoforms ( $M_r$  40 and 66 kDa) detected in NK cell lysates. Specific analyses of isolated subcellular fractions would be needed to clarify these aspects and also to assess the possible involvement of phosphorylation-dephosphorylation mechanisms in the trafficking of PC-PLC isoforms, following either cytokine-induced NK activation and/or exposure to a target cell.

Comparative epifluorescence and flow cytometry analyses on either unfixed or fixed and permeabilized NK cells showed that there was a 2-fold increase in the amount of PC-PLC located on the outer cell surface of NK-activated, with respect to NK-resting cells. Since, however, the overall expression of PC-PLC in unstimulated and IL-2-stimulated NK cells was very similar (according to flow cytometry and immunoblotting experiments), it seems reasonable to conclude that the increase in PC-PLC exposed on the outer cell surface was accompanied by a decrease in the cytoplasmic

PC-PLC content. In agreement with this hypothesis, CLSM analyses showed that IL-2 activation induced a substantial fraction of PC-PLC to leave the MTOC and translocate along microtubules to the periphery of NK cells. However, following incubation of NK-activated cells with D609, most of the PC-PLC-rich particles reassembled in the Golgi region. This body of evidence supports the hypothesis that subcellular localization and function of PC-PLC are interdependent phenomena, regulated by lymphokine activation.

More detailed insight on the cellular mechanisms of PC-PLC translocation in NK-activated cells and their involvement in NK cytotoxicity was provided by dual fluorescence CLSM evidence on the colocalization of this enzyme with 1) cytoskeleton components ( $\beta$ -tubulin and F-actin); 2) microtubule motor proteins (kinesin and dynein); 3) perforin-containing granules. In particular, these experiments showed that PC-PLC-rich particles were essentially clustered within the MTOC region of NK-resting cells and, following IL-2-activation, were massively transported toward the cell periphery, where they colocalized with F-actin in subcortical membrane regions.

The prevalent association of PC-PLC with kinesin, rather than with dynein, further supported a net transport of the enzyme in NK-activated cells, along microtubules, toward the plasma membrane. Kinesin and dynein are in fact held responsible for vesicle transport in opposite directions, under the control of phosphatases and kinases (34), the former supporting vesicle motility toward the fast-growing ends of microtubules, and the latter mainly supporting movements from cell periphery to the MTOC.

Finally, the extensive colocalization of cytoplasmic PC-PLC with perforin-containing lytic granules in NK-activated cells and the joint translocation of these molecular components from the Golgi complex to cell periphery clearly occurred along common migration routes made available by the microtubule organization. This overall body of evidence supports the participation of PC-PLC in the regulated mechanisms of lytic granule exocytosis, the major mechanism by which NK cells express their cytotoxic activity toward NK-sensitive targets (35). It is in fact known that, upon binding to a target cell, the cross-linking of specific surface receptors triggers in the effector cell a rapid reorganization of the cytoskeletal apparatus, resulting into a strong polarization of the MTOC, the Golgi complex, and perforin-containing lytic granules in the direction of the bound target. Once this polarity is established, the lytic granules translocate from the MTOC to the plasma membrane and finally release their lytic content of perforin and granzymes to the space between the effector and the target cell (Ref. 36 and references therein). Furthermore, studies on lytic granules isolated from CTLs demonstrated that the movement of these organelles along microtubules was mainly supported by kinesin, rather than by cytoplasmic dynein (Ref. 36 and references therein). The additional evidence provided by the present study on the colocalization of perforin-containing lytic granules with PC-PLC, their kinesin-supported cotransport along microtubule filaments of NK-activated cells, and, finally, their massive joint accumulation at the intercellular contact region of effector-target cell conjugates, strongly supports the hypothesis that PC-PLC plays a relevant role in the still scarcely elucidated mechanisms of lytic granule externalization.

Further insight on the involvement of PC-PLC in NK-mediated cytotoxicity was given by the strong dose-dependent decrease in NK-mediated lytic activity, following preincubation of the effector cell with D609. This xanthate compound is reported to inhibit PLC-mediated PC hydrolysis, without inducing any substantial modification of phospholipase A<sub>2</sub>, or D, or PI-PLC activities (22, 28, 29). For this reason, D609 has been utilized in a number of

intact cell systems to discriminate between different reaction steps in signal transduction cascades occurring in cell stimulated by either mitogens or apoptotic agents (17, 37, 38). It should, however, be explicitly noted that PC-PLC inhibition by D609 is not necessarily associated with an overall decrease of PC hydrolysis in treated cells. In fact, in a cell exposed to D609-mediated inhibition of PC-PLC, concomitant alterations can occur in the activity of other enzymes of the PC cycle, such as a (likely compensatory) increase in PC-pld activity, as reported for osteoblastic osteosarcoma cells (39) and fibroblasts (40). Recent studies also demonstrated that D609 inhibits sphingomyelin synthase *in vitro* and in SV40-transformed cells (41), suggesting that this compound may generally compete with PCho-containing substrates. Furthermore, PC-PLC inhibition by D609 may also interfere with the signal transduction cascade, by blocking mitogen-activated protein kinase activation, in response to some receptor-stimulating agents (39, 40). These observations point to the interest of directly measuring PC-PLC activity by appropriate biochemical analyses on cells and their subcellular fractions, to elucidate the specific role of this enzyme in the activation of the PC cycle and signal transduction mechanisms, in NK-mediated cytotoxicity. At the present stage, the new message provided by our immunofluorescence and microscopy data was that D609-induced decreases in NK cytotoxicity were associated with extensive reorganization of subcellular PC-PLC distribution, with both a reduction (up to 40%) in the fraction of the enzyme exposed on the outer membrane surface and clustering of the cytoplasmic fraction within the Golgi region. This evidence suggests a possible mode of action of D609, based upon a decrease of PC-PLC translocation from cytoplasmic granular components to the cell surface. The hypothesis reinforces the interest of further investigating, using appropriate biochemical assays, the relationships between activity and subcellular localization of PC-PLC in NK cells, under different conditions of preincubation with D609, cytokine-induced activation, and/or exposure to either sensitive or resistant target cells.

In conclusion, although indirect evidence demonstrates the involvement of PC-PLC in the activation of receptor-stimulated signal transduction mechanisms (19, 42, 43), only a few studies to date provided direct evidence on expression and subcellular localization of this enzyme in mammalian cells (25, 26, 44–46). The present work reported new evidence on the presence and subcellular distribution of PC-PLC in NK cells, supporting a previously unsuspected role of this enzyme in NK-mediated cytotoxicity. The specific biochemical and cellular mechanisms by which PC-PLC participates in NK granule exocytosis and target cell membrane lysis are still open questions, currently under investigation in our laboratories.

## Acknowledgments

We thank Dr. G. Trinchieri, Dr. R. Strom, and Dr. M. Sargiacomo for scientific discussions; Dr. B. Barletta for kindly providing purified anti-PC-PLC Abs; and S. Ramoni for expert preparation of the figures.

## References

- Trinchieri, G. 1989. Biology of natural killer cells. *Adv. Immunol.* 47:187.
- Krähenbühl, O., and J. Tschopp. 1991. Perforin-induced pore formation. *Immunol. Today* 12:399.
- Leibson, P. J. 1997. Signal transduction during natural killer cell activation: inside the mind of a killer. *Immunology* 6:655.
- Liscovitch, M. 1992. Crosstalk among multiple signal-activated phospholipases. *Trends Biochem. Sci.* 17:393.
- Liscovitch, M., and L. C. Cantley. 1994. Lipid second messengers. *Cell* 77:329.
- Roth, M. G., and P. C. Sternweis. 1997. The role of lipid signalling in constitutive membrane traffic. *Curr. Opin. Cell Biol.* 9:519.
- Windebank, K. P., R. T. Abraham, G. Powis, R. A. Olsen, T. J. Barna, and P. J. Leibson. 1988. Signal transduction during human natural killer cell activation: inositol phosphate generation and regulation by cyclic AMP. *J. Immunol.* 141:3951.
- Cassatella, M. A., I. Anegón, M. C. Cuturi, P. Grisley, G. Trinchieri, and B. Perussia. 1989. Fc $\gamma$ R (CD16) interaction with ligand induces Ca<sup>2+</sup> mobilization and phosphoinositide turnover in human natural killer cells: role of Ca<sup>2+</sup> in Fc $\gamma$ R (CD16)-induced transcription and expression of lymphokine genes. *J. Exp. Med.* 169:549.
- Brahmi, Z. 1992. Signal transduction mechanisms in NK cell cytotoxicity. In *NK Cell-Mediated Cytotoxicity: Receptors, Signaling and Mechanisms*. E. Lotzova and R. B. Herberman, eds. CRC Press, Boca Raton, p. 117.
- Ting, A. T., L. M. Karnitz, R. A. Schoon, R. T. Abraham, and P. J. Leibson. 1992. Fc $\gamma$  receptor activation induces the tyrosine phosphorylation of both phospholipase C (PLC)- $\gamma$ 1 and PLC- $\gamma$ 2 in natural killer cells. *J. Exp. Med.* 176:1751.
- Balboa, M. A., J. Balsinde, J. Aramburu, F. Mollinedo, and M. Lopez-Botet. 1992. Phospholipase D activation in human natural killer cells through the Kp43 and CD16 surface antigens takes place by different mechanisms: involvement of the phospholipase D pathway in tumor necrosis factor  $\alpha$  synthesis. *J. Exp. Med.* 176:9.
- Milella, M., A. Gismondi, P. Roncaioli, G. Palmieri, S. Morrone, M. Piccoli, L. Frati, M. G. Cifone, and A. Santoni. 1999.  $\beta$ <sub>1</sub> integrin cross-linking inhibits CD16-induced phospholipase D and secretory phospholipase A<sub>2</sub> activity and granule exocytosis in human NK cells: role of phospholipase D in CD16-triggered degranulation. *J. Immunol.* 162:2064.
- Piomelli, D. 1993. Arachidonic acid in cell signalling. *Curr. Opin. Cell Biol.* 5:274.
- Milella, M., A. Gismondi, P. Roncaioli, L. Bisogno, G. Palmieri, L. Frati, M. G. Cifone, and A. Santoni. 1997. CD16 cross-linking induces both secretory and extracellular signal-regulated kinase (ERK)-dependent cytosolic phospholipase A<sub>2</sub> (PLA<sub>2</sub>) activity in human natural killer cells: involvement of ERK, but not PLA<sub>2</sub>, in CD16-triggered granule exocytosis. *J. Immunol.* 158:3148.
- Cifone, M. G., P. Roncaioli, L. Cironi, C. Festuccia, A. Meccia, S. D'Alò, D. Botti, and A. Santoni. 1997. NKR-PIA stimulation of arachidonate-generating enzymes in rat NK cells is associated with granule release and cytotoxic activity. *J. Immunol.* 159:309.
- Diaz-Laviada, I., P. Larrodera, M. T. Diaz-Meco, M. E. Cornet, P. H. Guddal, T. Johansen, and J. Moscat. 1990. Evidence for a role of phosphatidylcholine-hydrolysing phospholipase C in the regulation of protein kinase C by *ras* and *src* oncogenes. *EMBO J.* 9:3907.
- Schütze, S., K. Pothoff, T. Machleidt, D. Berkovic, K. Wiegmann, and M. Krönke. 1992. TNF activates NF- $\kappa$ B by phosphatidylcholine-specific phospholipase C-induced "acidic" sphingomyelin breakdown. *Cell* 71:765.
- Xu, X. X., T. G. Tessner, C. O. Rock, and S. Jackowski. 1993. Phosphatidylcholine hydrolysis and *c-myc* expression are in collaborating mitogenic pathways activated by colony-stimulating factor. *J. Mol. Cell Biol.* 13:1522.
- Divecha, N., and R. F. Irvine. 1995. Phospholipid signaling. *Cell* 80:269.
- Halstead, J., K. Kemp, and R. A. Ignatz. 1995. Evidence for the involvement of phosphatidylcholine-phospholipase C and protein kinase C in transforming growth factor- $\beta$  signaling. *J. Biol. Chem.* 270:13600.
- Cowen, D. S., R. S. Sowers, and D. R. Manning. 1996. Activation of a mitogen-activated protein kinase (ERK2) by the 5-hydroxytryptamine 1A receptor is sensitive not only to inhibitors of phosphatidylinositol 3-kinase, but to an inhibitor of phosphatidylcholine hydrolysis. *J. Biol. Chem.* 271:22297.
- Wooten, D. K., T. K. Teague, and B. W. McIntyre. 1999. Separation of integrin-dependent adhesion from morphological changes based on differential PLC specificities. *J. Leukocyte Biol.* 65:127.
- Yue, C. C., C. W. Reynolds, and P. A. Henkart. 1987. Inhibition of cytolysin activity in large granular lymphocyte granules by lipids: evidence for a membrane insertion mechanism of lysis. *Mol. Immunol.* 24:647.
- Tschopp, J., S. Schafer, D. Masson, M. C. Peitsch, and C. Heusser. 1989. Phosphorylcholine acts as a Ca<sup>2+</sup>-dependent receptor molecule for lymphocyte perforin. *Nature* 337:272.
- Clark, M. A., R. G. L. Shorr, and J. S. Bomalaski. 1986. Antibodies prepared to *Bacillus cereus* phospholipase C crossreact with a phosphatidylcholine preferring phospholipase C in mammalian cells. *Biochem. Biophys. Res. Commun.* 140:114.
- Podo, F., A. Ferretti, A. Knijn, P. Zhang, C. Ramoni, B. Barletta, C. Pini, S. Baccarini, and S. Pulciani. 1996. Detection of phosphatidylcholine-specific phospholipase C in NIH-3T3 fibroblasts and their H-*ras* transformants: NMR and immunochemical studies. *Anticancer Res.* 16:1399.
- Perussia, B., C. Ramoni, I. Anegón, M. C. Cuturi, J. Faust, and G. Trinchieri. 1987. Preferential proliferation of natural killer cells among peripheral blood mononuclear cells co-cultured with B lymphoblastoid cell lines. *Nat. Immun. Cell Growth Regul.* 6:171.
- Müller-Decker, K. 1989. Interruption of TPA-induced signals by an antiviral and antitumoral xanthate compound: inhibition of a phospholipase C-type reaction. *Biochem. Biophys. Res. Commun.* 162:198.
- Amtmann, E. 1996. The antiviral, antitumoral xanthate D609 is a competitive inhibitor of phosphatidylcholine-specific phospholipase C. *Drugs Exp. Clin. Res.* 22:287.
- Sabnis, R. W., T. G. Deligeorgiev, M. N. Jachak, and T. S. Dalvi. 1997. DiOC<sub>6</sub>(3): a useful dye for staining the endoplasmic reticulum. *Biotech. Histochem.* 72:253.
- D'Santos, C. S., J. H. Clarke, R. F. Irvine, and N. Divecha. 1999. Nuclei contain two differentially regulated pools of diacylglycerol. *Curr. Biol.* 9:437.
- Raben, D. M., and J. J. Baldassarre. 2000. Nuclear envelope signaling-role of phospholipid metabolism. *Eur. J. Histochem.* 44:67.
- Cocco, L., A. M. Martelli, R. S. Gilmour, S. G. Rhee, and F. A. Manzoli. 2001. Nuclear phospholipase C and signaling. *Biochim. Biophys. Acta* 1530:1.



34. Reese, E. L., and L. T. Haimo. 2000. Dynein, dynactin, and kinesin II's interaction with microtubules is regulated during bidirectional organelle transport. *J. Cell Biol.* 151:155.
35. Henkart, P. A. 1985. Mechanisms of lymphocyte-mediated cytotoxicity. *Annu. Rev. Immunol.* 3:31.
36. Burkhardt, J. K., J. M. McIlvain, Jr., M. P. Sheetz, and Y. Argon. 1993. Lytic granules from cytotoxic T cells exhibit kinesin-dependent motility on microtubules in vitro. *J. Cell Sci.* 104:151.
37. Kiss, Z., K. S. Crilly, and T. Chung. 1998. Stimulation of DNA synthesis in untransformed cells by the antiviral and antitumoral compound tricyclodecan-9-yl-xanthogenate (D609). *Biochem. Pharmacol.* 55:915.
38. Cifone, M. G., P. Rocaioli, R. De Maria, G. Camarda, A. Santoni, G. Ruberti, and R. Testi. 1995. Multiple pathways originated at the Fas/Apo-1 (CD95) receptor: sequential involvement of phosphatidylcholine-specific phospholipase C and acidic sphingomyelinase in the propagation of the apoptotic signal. *EMBO J.* 14:5859.
39. Singh, A. T. K., J. M. Radeff, J. G. Kunnel, and P. H. Stern. 2000. Phosphatidylcholine-specific phospholipase C inhibitor, tricyclodecan-9-yl xanthogenate (D609), increases phospholipase D-mediated phosphatidylcholine hydrolysis in UMR-106 osteoblastic osteosarcoma cells. *Biochim. Biophys. Acta* 1487:201.
40. Van Dijk, M. C. M., F. J. G. Muriana, J. De Widt, H. Hilkmann, and W. J. van Blitterswijk. 1997. Involvement of phosphatidylcholine-specific phospholipase C in platelet-derived growth factor-induced activation of the mitogen-activated protein kinase pathway in Rat-1 fibroblasts. *J. Biol. Chem.* 272:11011.
41. Luberto, C., and Y. A. Hannun. 1998. Sphingomyelin synthase, a potential regulator of intracellular levels of ceramide and diacylglycerol during SV40 transformation: does sphingomyelin synthase account for the putative phosphatidylcholine-specific phospholipase C? *J. Biol. Chem.* 273:14550.
42. Pelech, S. L., and D. E. Vance. 1989. Signal transduction via phosphatidylcholine cycles. *Trends Biochem. Sci.* 14:28.
43. Exton, J. H. 1994. Phosphatidylcholine breakdown and signal transduction. *Biochim. Biophys. Acta* 1212:28.
44. Wolf, R. A., and R. W. Gross. 1985. Identification of neutral active phospholipase C which hydrolyzes choline glycerophospholipids and plasmalogen selective phospholipase A<sub>2</sub> in canine myocardium. *J. Biol. Chem.* 260:7295.
45. Sheikhejad, R. G., and P. N. Srivastava. 1986. Isolation and properties of a phosphatidylcholine-specific phospholipase C from bull seminal plasma. *J. Biol. Chem.* 261:7544.
46. Ferretti, A., F. Podo, G. Carpinelli, L. L. Chen, P. Borghi, and R. Masella. 1993. Detection of neutral active phosphatidylcholine-specific phospholipase C in Friend leukemia cells before and after erythroid differentiation. *Anticancer Res.* 13:2309.